

Article

Decrease in the Starting Temperature of the Reaction for Fabricating Carbides of Refractory Metals When Using Carbon Nanoparticles as Precursors

Vladimir Popov ^{1,*}, Anna Borunova ², Evgeny Shelekhov ¹, Oksana Koplak ³, Elizaveta Dvoretzkaya ³, Danila Matveev ⁴, Alexey Prosviryakov ¹, Ekaterina Vershinina ⁵ and Vladimir Cheverikin ¹

- ¹ Department of Physical Metallurgy of Non-ferrous Metals, National University of Science and Technology "MISIS", 119049 Moscow, Russia
- ² N.N. Semenov Federal Research Center for Chemical Physics of Russian Academy of Sciences, 119334 Moscow, Russia
- ³ Federal Research Center of Problems of Chemical Physics and Medicinal Chemistry of Russian Academy of Sciences, 142432 Chernogolovka, Russia
- ⁴ Osipyan Institute of Solid State Physics of Russian Academy of Sciences, 142432 Chernogolovka, Russia
- ⁵ Department of Innovative Materials and Corrosion Protection, Dmitry Mendeleev University of Chemical Technology of Russia, 125047 Moscow, Russia
- * Correspondence: popov58@inbox.ru



Citation: Popov, V.;

Borunova, A.; Shelekhov, E.;
Koplak, O.; Dvoretzkaya, E.;
Matveev, D.; Prosviryakov, A.;
Vershinina, E.; Cheverikin, V.

Decrease in the Starting Temperature of the Reaction for Fabricating Carbides of Refractory Metals When Using Carbon Nanoparticles as Precursors. *Inventions* **2022**, *7*, 120. <https://doi.org/10.3390/inventions7040120>

Academic Editor: Zhengyi Jiang

Received: 10 November 2022

Accepted: 7 December 2022

Published: 12 December 2022

Publisher's Note: MDPI stays neutral with regard to jurisdictional claims in published maps and institutional affiliations.



Copyright: © 2022 by the authors. Licensee MDPI, Basel, Switzerland. This article is an open access article distributed under the terms and conditions of the Creative Commons Attribution (CC BY) license (<https://creativecommons.org/licenses/by/4.0/>).

Abstract: Metal matrix composites with a matrix of refractory metals (niobium, tungsten) and reinforcing nanodiamond particles were prepared for studying the possibility of decreasing the starting temperature of carbide synthesis. The size of primary nanodiamond particles was 4–6 nm, but they were combined in large-sized agglomerates. Mechanical alloying was used for producing the composites by crushing agglomerates and distributing nanodiamonds evenly in the metal matrix. The initial and fabricated materials were investigated by X-ray diffraction, differential scanning calorimetry, and transmission and scanning electron microscopy. Thermal processing leads to the reaction for carbide synthesis. Studies have found that the usage of carbon nanoparticles (nanodiamonds) as precursors for fabricating carbides of refractory metals leads to a dramatic decrease in the synthesis temperature in comparison with macro-precursors: lower than 200 °C for tungsten and lower than 350 °C for niobium.

Keywords: metal matrix nanocomposites; nanodiamonds; carbides of refractory metals; mechanical alloying; in situ synthesis

1. Introduction

In recent years, interest in carbon nanoparticles and their applications in many fields of science and technology has grown [1–4]; examples include fullerenes and carbon onions [5–7]. There are many studies of detonation synthesis nanodiamonds [8–11]. Like all nanopowders, nanodiamonds are subject to agglomeration, and combine into large aggregates. The size of primary nanodiamond particles is 4–6 nm (a small portion of them reach 10 nm) [12], but they are all combined in agglomerates, which can reach millimeters in size (Figure 1). Bonds in agglomerates are weaker in comparison with the monolithic material. If the agglomerate is placed in a metal matrix composite, it will be destroyed by the application of load. This can lead to the destruction of the whole material because of the generation of the stress concentrator. On the other hand, during in situ synthesis (i.e., the chemical reaction of nanodiamonds with the material of the matrix) if there are agglomerates of nanoparticles, large-sized carbide particles will be formed. This will lead to a reduction in the effect of using carbon nanoparticles. It will be necessary to crush the agglomerates. This article is focused on studying the opportunity to decrease the starting temperature of the reaction for fabricating carbides of refractory metals when using carbon nanoparticles as precursors.

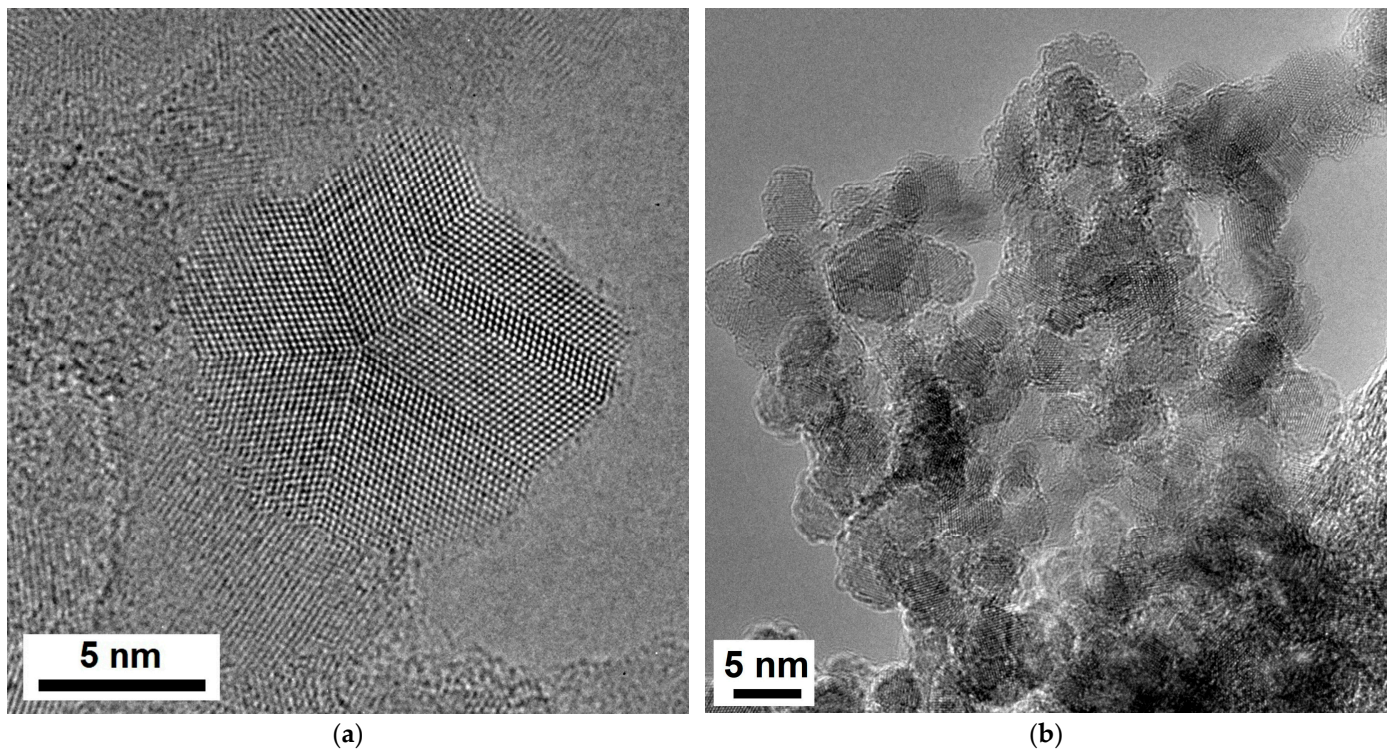


Figure 1. TEM images of nanodiamonds: (a) prime nanoparticle with twins; (b) agglomeration of nanodiamonds.

Refractory metals are of much interest for use in the engineering of many spheres [13–15]. Carbides of niobium [16–22] and tungsten [23–28] are also of interest to the industry. One of problems in fabricating these carbides is the necessity for high synthesis temperatures (1400–2000 °C) during the reaction between the metal (or its oxide) and carbon [29,30]. There are methods to fabricate carbides of refractory metals at lower temperatures, but they all relate to using intermediate and auxiliary chemical compounds, which have an adverse effect on the fineness [31]. That is why designing methods for fabricating carbides of various metals during the direct chemical reaction between the metal and carbon is a vital task. The opportunity to decrease the carbide synthesis temperature when using carbon nanoparticles as precursors has been studied in several works: articles show that the use of carbon nanoparticles (nanodiamonds [9,32], fullerenes, carbon onions [6], globular carbon [3]) in aluminum matrix composites leads to the synthesis of aluminum carbides at significantly lower temperatures than in the case of macro-materials: when fullerenes are used, the decrease reaches 350 °C. This effect was also investigated when using chromium as a composite matrix with nanodiamond reinforcing particles [33]. The temperature was reduced to 520 °C. Studies of using this effect for the synthesis of refractory metal carbides are important, since the existing methods of producing such carbides use high temperatures. Reducing the synthesis temperature will lead to a significant economic effect (reducing energy costs, costs of equipment, and usage of expensive high-temperature materials) and improve the environmental situation.

2. Materials, Equipment, and Research Methods

Commercially available powders of niobium and tungsten (supplied by VILS, Moscow, Russia) were used as the base material for fabricating the matrix of composite materials. Niobium powder contained 3%_wt of niobium hydride, which was formed as a result of long-term storage at technical premises (niobium actively reacts with hydrogen); other impurities in total were not more than 0.35%_wt (Table 1). Niobium particles had sizes of 10–50 microns. Total impurities in tungsten powder were not more than 0.5 %_wt (Table 2). Tungsten particles had sizes of 0.5–3 microns.

Table 1. Chemical composition of the niobium powder.

Element	Ta	Si	Fe	W	Mo	C	NbH	Other Impurities	Nb
Content, % _{mass}	0.05	0.03	0.02	0.02	0.02	0.1	3.0	0.11	Balance

Table 2. Chemical composition of the tungsten powder.

Element	Fe	Ni	Mo	K	Na	C	Other Impurities	W
Content, % _{mass}	0.1	0.06	0.1	0.02	0.02	0.1	0.1	Balance

Commercially available powder of nanodiamonds from detonation synthesis, supplied by Elektrokhimkomplekt (Ekaterinburg, Russia), were chosen as reinforcing particles. Powder contained diamond phase not less than 95.0%_{wt}. The composite material was fabricated by a mechanical alloying method, i.e., the processing of primary mixtures in planetary mills [34–37]. A Pulverisette 6 planetary mono-mill (FRITSCH GmbH, Germany) was used. The grinding jar had a volume of 80 mL and chromium steel balls (100 g) with a diameter of 5 mm were used as the grinding tool. Rotation speed was equal to 500 rpm. The processing has been implemented without any surfactants in an argon atmosphere for 0.5–9 h; the shut-down period for cooling was not included in the total processing time. Information about fabricated composites is presented in Table 3 (Digital Jewelry Scale FC-50 was used to weigh materials).

Table 3. Composite materials fabricated using mechanical alloying.

Number of Specimen	Type and Mass of Metal, g	Mass of Nanodiamonds, g	Content of Nanodiamonds, % _{mass}	Time of Mechanical Alloying, h
1-Nb	Nb, 9.296	0.653	6.56	0.5
2-Nb	Nb, 9.302	0.699	6.98	1.2
3-Nb	Nb, 9.307	0.699	6.98	6
4-W	W, 20.092	0.653	3.25	9

The fabricated powdery granules underwent a detailed study with the help of scanning electron microscopy (SEM), X-ray diffraction (XRD), and differential scanning calorimetry (DSC) [38–42], which was carried out on two appliances: DSC 404 C Pegasus and STA 449 F3 Jupiter (both manufactured by NETZSCH, Germany). In both cases, the heating rate was 20 degrees per minute. A DSC 404 C Pegasus was used for studying the niobium composites under heating up to 1000–1400 °C. Results were measured in an argon atmosphere with the feed rate of 50 mL/min. The appliance was graduated for measuring in mW/mg. An STA 449 F3 Jupiter was used for studying the tungsten composites under heating up to 1550 °C. Results were measured in a helium atmosphere with a feed rate of 50 mL/min. This appliance allowed us to perform differential scanning calorimetry (DSC) with the registration in microvolts and thermal gravimetric analysis (TG). Air was evacuated from the working chamber for the graduating scales. The working chamber was filled-in with helium of 6.0 mark (99.9999%). Thereafter, the appliance was returned to the original state. Two empty closed alumina (Al₂O₃) crucibles were then placed on the holder inside the working chamber of the appliance. The procedure of evacuation and filling-in was repeated, the baseline for the empty crucible was recorded and the appliance was returned to the original state. Then, the investigating sample was placed into one of the empty crucibles, the procedure of evacuation and filling-in was repeated, and necessary measurements were performed. The results of the DSC and TG of the sample were compared with the results of the empty crucible, considering the baseline for the empty crucible. The X-ray diffraction analysis was conducted using an X-ray diffractometer DRON-3 (Russia, Saint-Petersburg) with CuK α radiation. Reference [43] provides information about the technique and the

software used during X-ray diffraction studies. During the phase analysis, data from ICSD (Inorganic Crystal Structure Database), CRYSTMET, COD (Crystallography Open Database) bases were used. A scanning electron microscope TESCAN VEGA3 (Czech Republic, Brno-Kohoulovice) and Supra 50VP (Carl Zeiss, Germany) was used for examining the general appearance of granules and their surface. Transmission electron microscopy studies were performed using a TITAN 80–300 (FEI, International).

3. Results and Discussion

Composite materials of «niobium + nanodiamonds» and «tungsten + nanodiamonds» (Table 1) were fabricated using mechanical alloying. Approximately, niobium composites contain 7%_{mass} of nanodiamonds, and tungsten composites contain 3%_{mass} of nanodiamonds. Niobium has decreased strength in comparison with tungsten, which is why it was applied for the investigation of several treatment periods of mechanical alloying: (i) short time—0.5 h (specimen 1-Nb), (ii) middle time—1.2 h (specimen 2-Nb); (iii) long time—6 h (specimen 3-Nb). The high strength of tungsten is the reason for the use of a long treatment time in mechanical alloying: 9 h (specimen 4-W).

3.1. Niobium Composites

The fabricated samples of composites were studied by scanning electron microscopy (SEM), X-ray diffraction (XRD), and differential scanning calorimetry (DSC). The general views of the initial niobium powder and niobium composite granules are presented in Figure 2a–d. During mechanical alloying, nanodiamond agglomerates are destroyed and mixed with metal particles, nanodiamond particles are embedded in a metal matrix, and metal particles are destroyed and welded again. Mixing, destruction, and welding processes lead to the formation of composite granules. The processing time determines the degree of destruction of primary nanodiamond agglomerates. The images in Figure 2 indicate that processing for a short time does not cause a high degree of elaboration of the structure (Figure 2b). An increase in the time of mechanical alloying leads to significant destruction of nanodiamond agglomerates, a decrease in the size of granules, and an increase in the uniformity of the material.

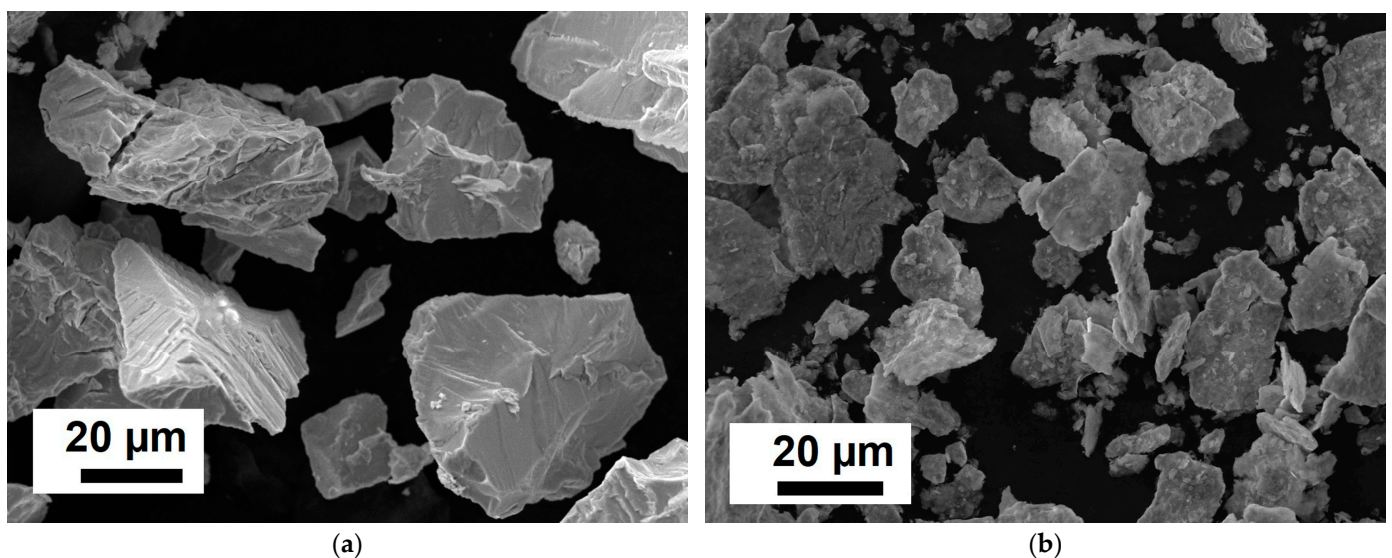


Figure 2. Cont.

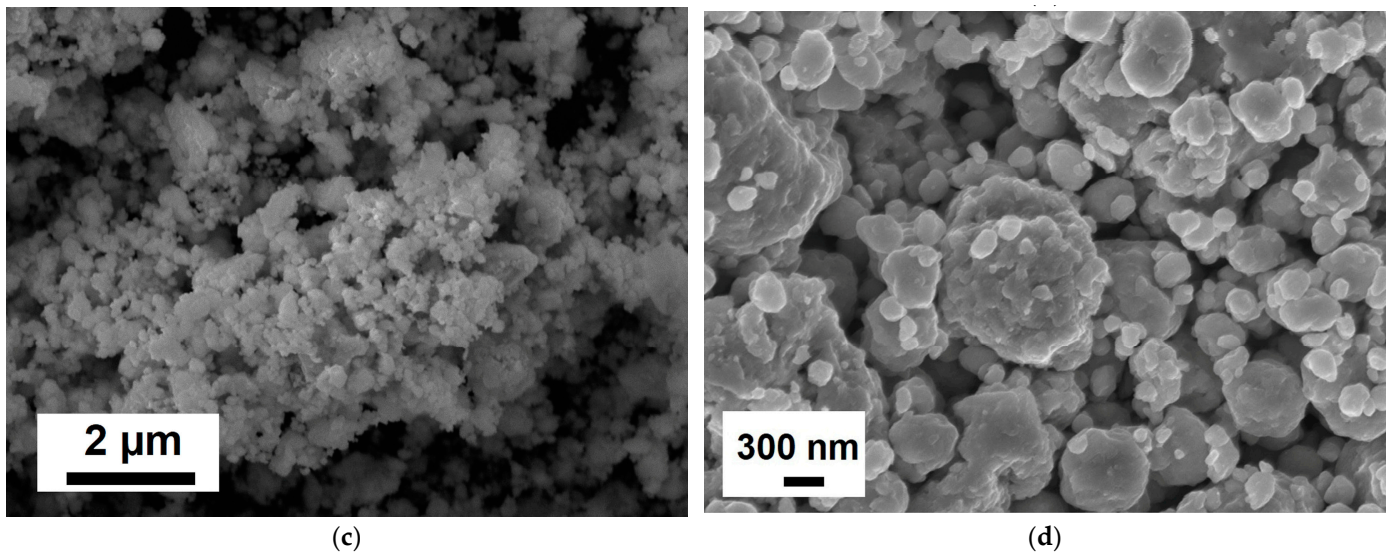


Figure 2. General view of the initial niobium powder (a) and composite granules “Nb + 7%_{mass}ND” after various treatment periods of mechanical alloying: (b) 0.5 h; (c) 1.2 h; (d) 6 h ((a–c) SEM TESCAN VEGA3; (d) SEM Supra 50VP).

X-ray diffraction analysis was performed for «niobium + nanodiamonds» composites fabricated after mechanical alloying for 0.5 h, 1.2 h, and 6 h. The results are presented in Figure 3.

As can be seen in the X-ray diffraction patterns, carbides are not fabricated practically if the time of processing is short. When processing for 0.5 h, hydrides, which were generated in niobium powder upon storage, did not decompose. After processing for 1.2 h, some number of carbides were observed. In samples processed by mechanical alloying for 6 h, a considerable proportion of nanodiamonds participated in the synthesis of niobium carbide. This can be explained by the fact that in the place where balls collide during the mechanical alloying, the temperature can reach and even exceed 400 °C [44]. To reduce this value, it is obviously necessary to use special methods (cryo-milling, etc.). Calculations show that not all carbon material reacted during the mechanical alloying. Hence, this sample has been studied further.

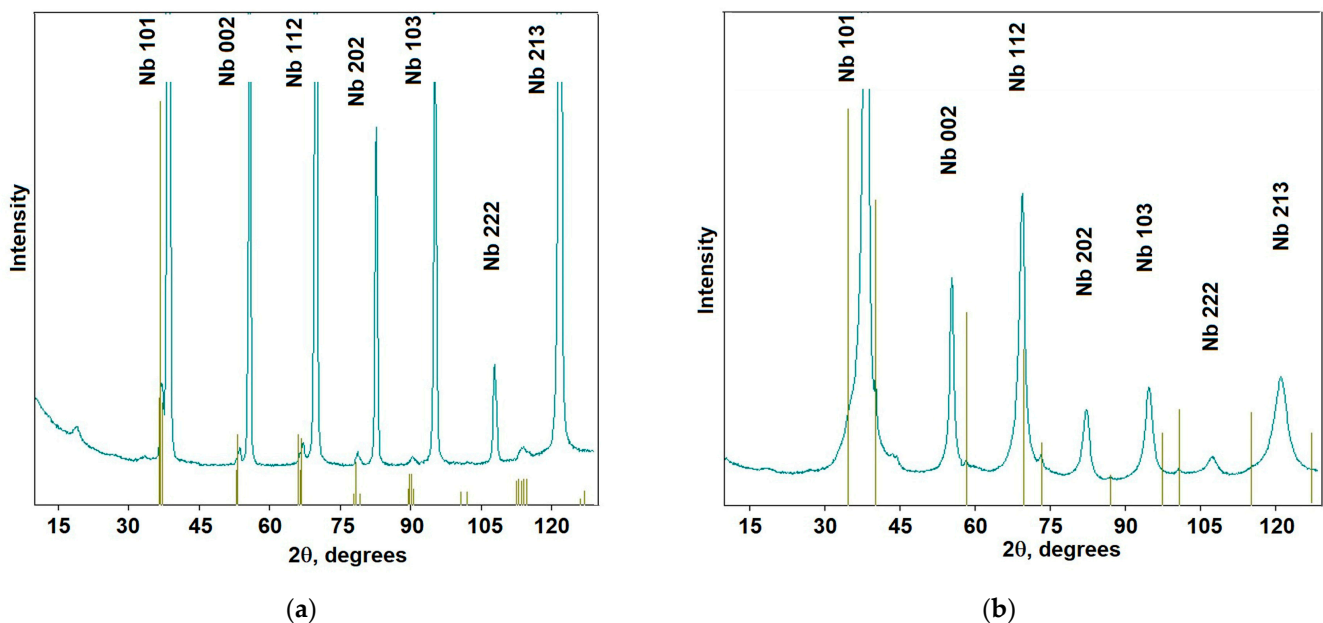


Figure 3. Cont.

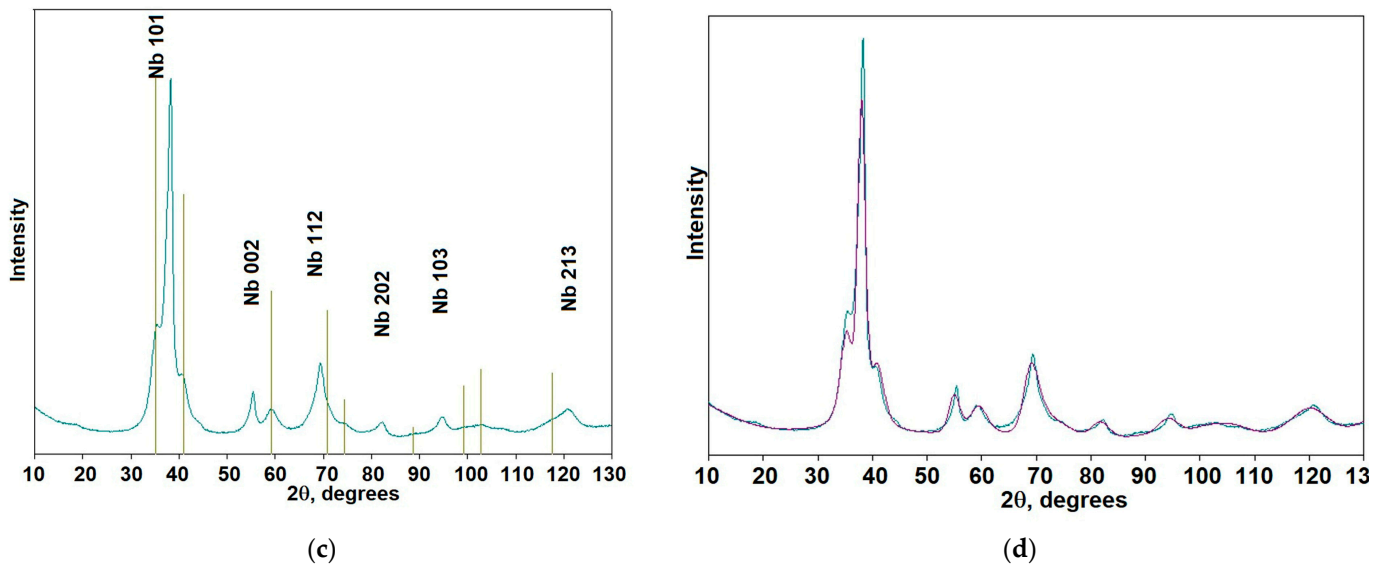


Figure 3. X-ray diffraction patterns of samples of the «niobium + nanodiamonds» composite after various processing times by mechanical alloying: (a) after 0.5 h (stick-diagram shows niobium hybrid $\text{NbH}_{0.86}$), (b) after 1.2 h (stick-diagram shows niobium carbide NbC), (c) after 6 h (stick-diagram shows niobium carbide $\text{NbC}_{0.77}$), (d) comparing the experimental X-ray diffraction pattern (painted green) with the fitted X-ray diffraction pattern (painted lilac) for the sample shown in Figure 3c.

An important part of the study was the differential scanning calorimetry of composite samples with a niobium matrix and nanodiamond reinforcing particles (Figure 4).

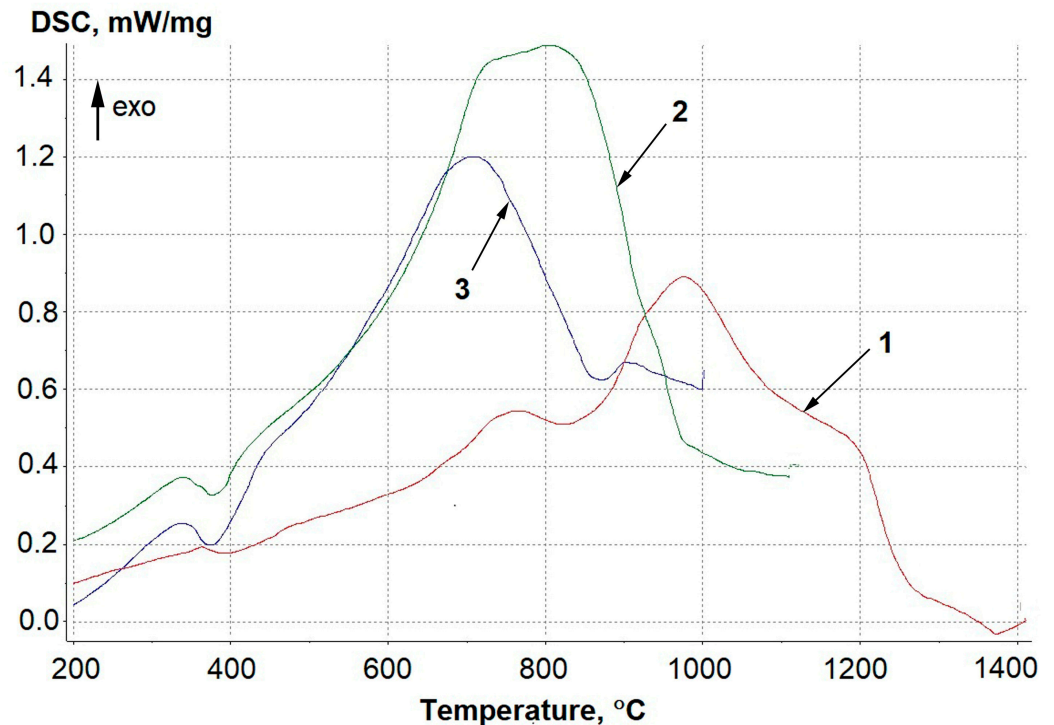


Figure 4. Results of DSC studies of samples of «niobium + nanodiamonds» composites: 1—after 0.5 h of processing (specimen 1-Nb); 2—after 1.2 h of processing (specimen 2-Nb); 3—after 6 h of processing (specimen 3-Nb).

A short processing time by mechanical alloying did not allow us to significantly crush the agglomerates of the nanodiamonds; hence, the maximum of peak heat release has

been observed at 950–1000 °C (Figure 4, curve 1 in red, specimen 1-Nb, processing time in the planetary mill was 0.5 h). A longer processing time leads to more serious crushing of agglomerates. As a result, the maximum of peak heat release shifts to a lower temperature: after 1.2 h of processing the maximum peak is approximately at 800 °C (Figure 4, curve 2 in green, specimen 2-Nb), and after 6 h of processing the maximum peak is approximately at 700 °C (Figure 4, curve 3 in blue, specimen 3-Nb). In all cases of using mechanical alloying, there are some fully crushed agglomerates. Consequently, heat release due to the fabrication of carbides has been observed even at 300–400 °C. To confirm the fabrication of carbides at heating, the XRD study of the sample processed for 6 h in the planetary mill (after heating up to 350–760 °C) was performed (Table 4).

Table 4. Content of phases in the sample processed in the planetary mill for 6 h after various thermal processing.

Temperature, °C	Phase	Volume Fraction, %	Mass Fraction, %
As milled	NbC _{0.77} (B1, cF8)	49.4	47.8
	Balance–Nb		
350	NbC _{0.77} (B1, cF8)	66.1	65.6
	Balance–Nb		
275	NbC _{0.77} (B1, cF8)	67.1	66.0
	Balance–Nb		
417	NbC _{0.77} (B1, cF8)	69.7	68.0
	Balance–Nb		
760	NbC _{0.77} (B1, cF8)	65.3	64.7
	Nb ₂ C (L'3, hP4)	8.0	8.1
	Nb ₂ C (oP12)	21.4	21.3
	Balance–niobium oxide		

Thus, the synthesis of niobium carbides begins at temperatures lower than 350 °C if carbon nanoparticles (in this case, nanodiamonds have been chosen) are used as precursors and if there is firm contact between components.

3.2. Tungsten Carbides

Figure 5 shows general views of the initial tungsten powder and tungsten composite granules.

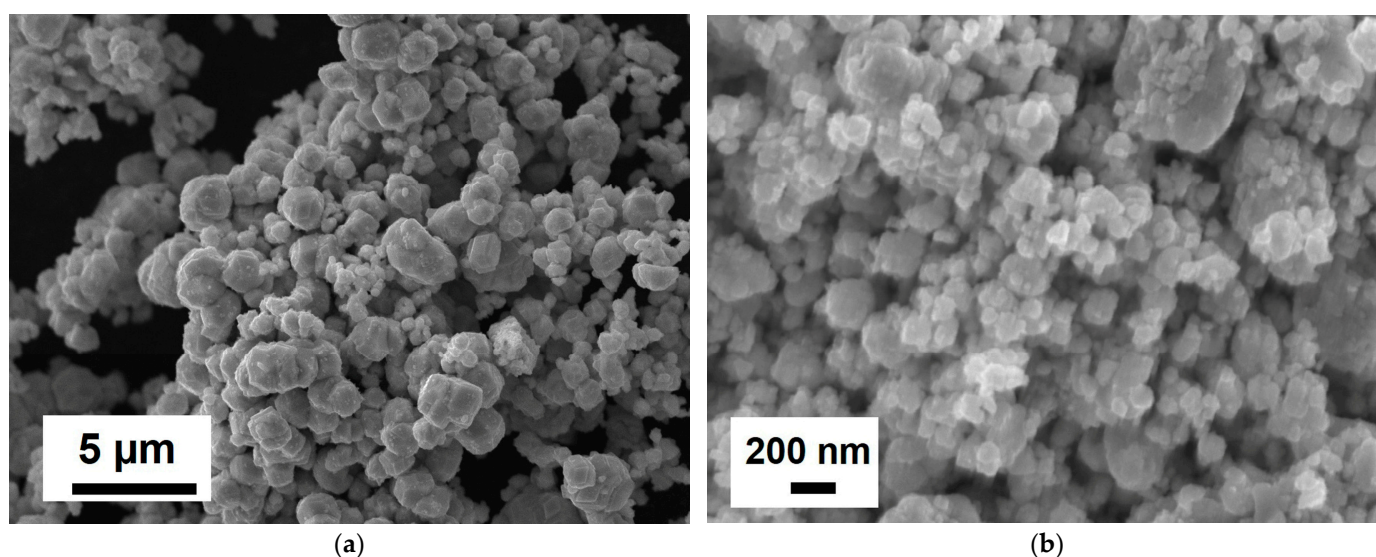


Figure 5. General view of initial tungsten powder (a) and composite granules (b). The general view of investigated tungsten materials: (a) tungsten initial powder (SEM NESCOAN VEGA3); (b) composite granules (SEM Supra 50VP).

Analysis by scanning electron microscopy revealed the smaller size of the tungsten particles. The X-ray diffraction patterns of the «tungsten + nanodiamonds» sample after mechanical alloying indicate that the sample mainly consists of tungsten (Figure 6a). The lower left part of the first peak indicates that there are some amorphous tungsten carbides in the composite after mechanical alloying. There is about 1% of tungsten oxide (WO_2) in the sample (Figure 6b), which has possibly been generated from adsorbed atmospheric oxygen in the initial powders. The X-ray diffraction analysis using traditional appliances does not allow us to determine carbon nanoparticles in the metal matrix. The explanation for this is described in reference [45]. Later (during heating) tungsten carbides will be formed. This indicates that carbon material (the nanodiamonds) exists in the composite.

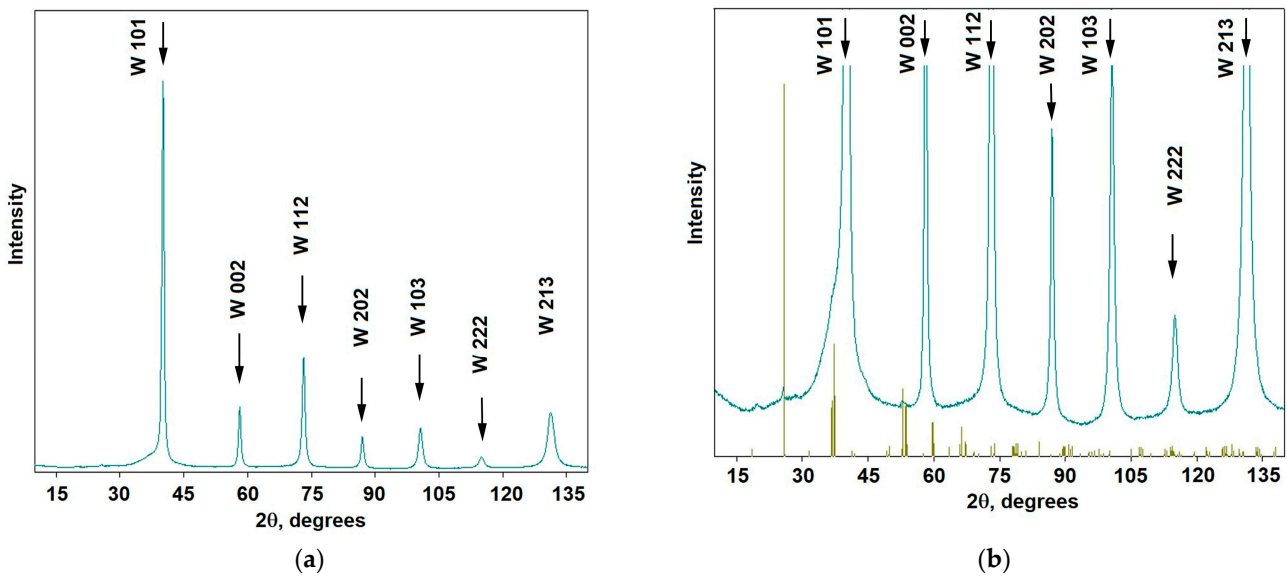


Figure 6. X-ray diffraction patterns of the composite material «tungsten + nanodiamonds»: (a) general view, (b) enlarged scale (tungsten peaks are shown with arrows, stick diagram shows tungsten oxide WO_2).

The most interesting analysis to perform is differential scanning calorimetry. Figure 7 shows the results of DSC studies of the «tungsten + nanodiamonds» composite.

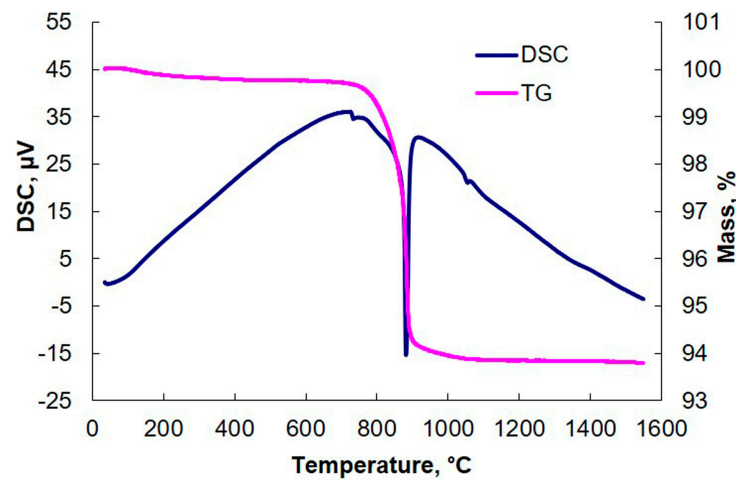


Figure 7. Results of differential scanning calorimetry (DSC) studies of the «tungsten + nanodiamonds» composite sample.

In Figure 7, the curve of DSC presents exo- and endo-peaks. The exo-peak is associated with heat release during the synthesis of tungsten carbides, the endo-peak is associated

with the sublimation of the oxide WO_3 [46,47]. X-ray diffraction studies prove the presence of carbides and oxides. Figure 8 shows results of XRD studies after heating up to 720 °C.

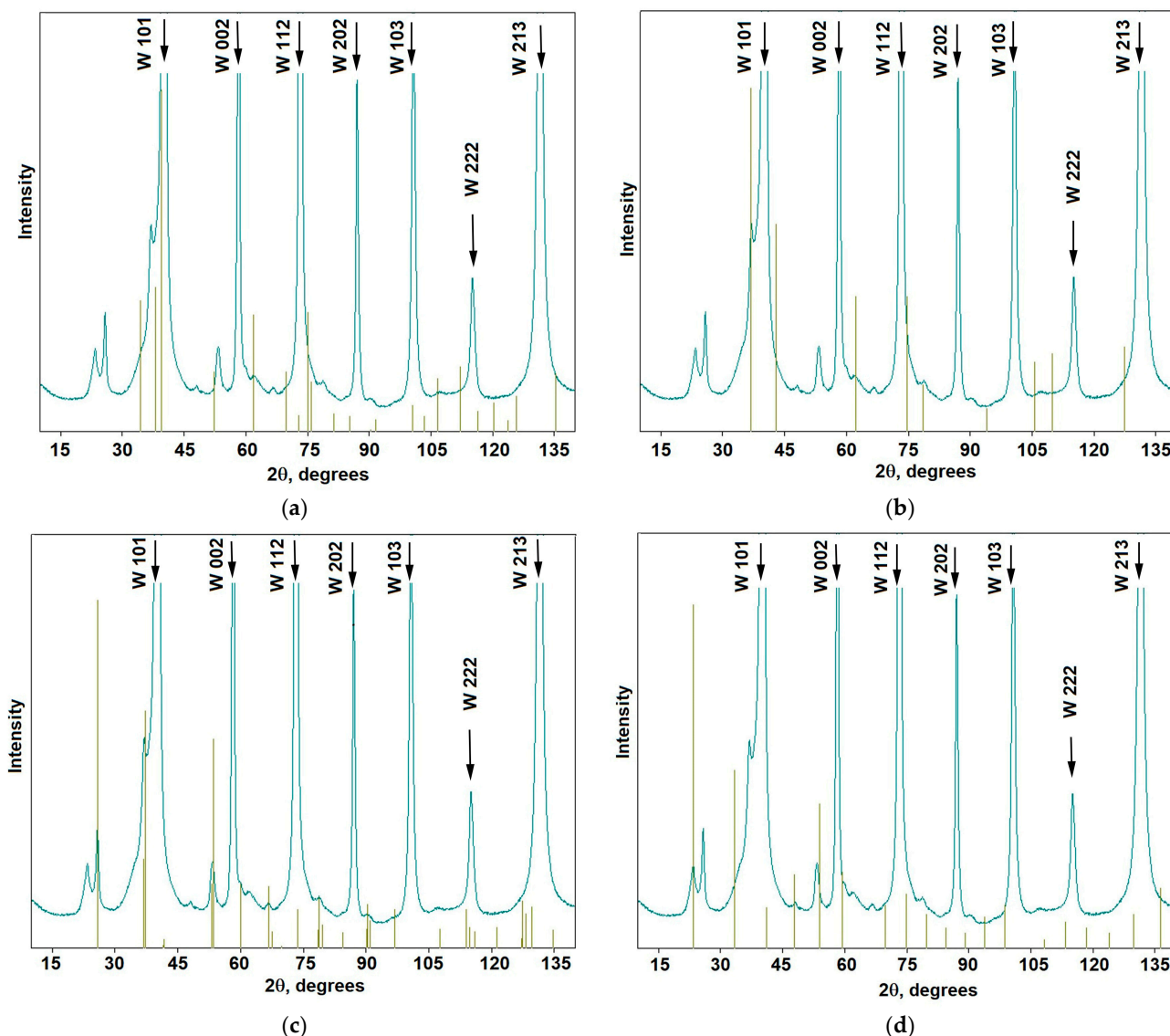


Figure 8. The X-ray diffraction pattern of the «tungsten + nanodiamonds» composite after heating up to 720 °C; tungsten peaks are shown with arrows, stick-diagrams show: (a) W_2C , (b) $WC_{0.82}$, (c) WO_2 , (d) WO_3 .

XRD analysis determined the presence of the following phases: W, W_2C , $WC_{0.82}$, WO_2 , and WO_3 . Table 5 presents shares of these phases in the sample determined using techniques described in the paper [43].

Table 5. Composition of the sample of the «tungsten + nanodiamonds» composite after heating to 720 °C.

Phase	Volume Fraction, %	Mass Fraction, %
W (A2, cI2)	61.2	69.0
W_2C (C6, hP3)	14.6	14.7
$WC_{0.82}$ (B1, cF8)	6.9	7.0
WO_2 (C4, tP6)	9.4	6.0
WO_3 (D0.9, cP4)	7.9	3.3

In comparison with the initial condition, tungsten carbides and oxide WO_3 have appeared; the content of oxide WO_2 has increased. It can be assumed that there was some oxygen in the initial powders in the adsorbed state. During further heating of the sample in DSC, endo-peak can be observed. This endo-peak is associated with the sublimation of oxide WO_3 . Sublimation is proved by the decrease in the sample mass and the results of the TG measurement (Figure 7). XRD analysis of the sample after heating up to $1000\text{ }^\circ\text{C}$ and $1600\text{ }^\circ\text{C}$ showed the presence of tungsten and tungsten carbide W_2C (Figure 9).

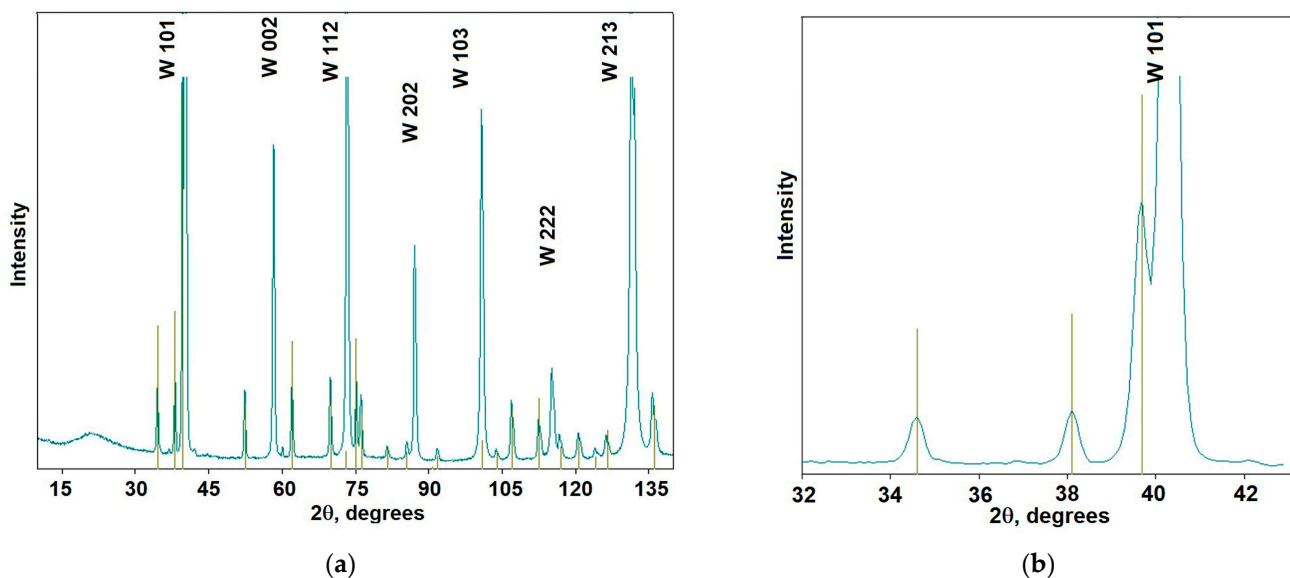


Figure 9. X-ray diffraction pattern of the «tungsten + nanodiamonds» composite after heating up to $1600\text{ }^\circ\text{C}$ (tungsten peaks are shown with arrows; the stick diagram shows lines of tungsten carbide W_2C): (a) general view (the amorphous halo is about 22° from the sample holder); (b) scaled-up section.

This means that oxide WO_2 transformed into oxide WO_3 and has fully sublimated, and carbide $WC_{0.82}$ transformed in carbide W_2C at carbon deficit.

However, the main result shown from these DSC studies is that the synthesis of tungsten carbides, when using nanodiamonds as precursors, begins even at temperatures below $200\text{ }^\circ\text{C}$.

Studies have shown that carbon nanoparticles react to synthesize carbides with metal in the matrix. There is in situ synthesis of niobium carbides in the niobium matrix and tungsten carbides in the tungsten matrix at the lower temperatures. Such technological operations lead to the formation of metal matrix composites with strengthening carbide nanoparticles of the metals from which the matrix is made.

4. Conclusions

The possibility of creating composites with a matrix of niobium or tungsten and reinforcing nanodiamond particles is shown. The use of differential scanning calorimetry and X-ray diffraction methods made it possible to establish that the application of nanodiamonds (nanosized carbon material) as a precursor for the synthesis of niobium and tungsten carbides leads to a decrease in the starting temperature of carbide formation: the synthesis of niobium carbides begins at temperatures below $350\text{ }^\circ\text{C}$ and that of tungsten carbides below $200\text{ }^\circ\text{C}$. The use of such a technological procedure will facilitate the production of composites with a matrix of refractory metals (niobium, tungsten) and reinforcing nanoparticles of niobium or tungsten carbides obtained by in situ synthesis directly in the composite matrix.

Author Contributions: Conceptualization, investigation, V.P.; mechanical alloying, A.B.; XRD analyses, E.S.; DSC analysis, O.K. and E.D.; SEM investigation, D.M. and V.C.; analysis of results, A.P., investigation, E.V. All authors have read and agreed to the published version of the manuscript.

Funding: This research received no external funding.

Data Availability Statement: Not applicable.

Acknowledgments: The authors are grateful to B. Senatulin, C. Kuebel, and Di Wang for assistance in the study.

Conflicts of Interest: The authors declare no conflict of interest.

References

1. Islam, A.; Sharma, V.K.; Mausam, K. An analytical study of nano carbon materials for developing metal matrix nano compo-sites. *Mater. Today Proc.* **2021**, *45*, 2867–2870. [[CrossRef](#)]
2. Tan, W.; Jiang, X.; Shao, Z.; Sun, H.; Fang, Y.; Shu, F. Fabrication and mechanical properties of nano carbon reinforced lam-inated Cu matrix composites. *Powder Technol.* **2022**, *395*, 377–390. [[CrossRef](#)]
3. Popov, V.; Borunova, A.; Shelekhov, E.; Khodos, I.; Senatulin, B.; Matveev, D.; Versinina, E. Peculiarities of chemical interaction of some carbon nanoreinforcements with aluminum matrix in metal matrix composite (MMC). *Mater. Werkst.* **2022**, *53*, 602–607. [[CrossRef](#)]
4. Reddy, S.T.; Manohar, H.; Anand, S. Effect of carbon black nano-fillers on tribological properties of Al6061-Aluminium metal matrix composites. *Mater. Today Proc.* **2019**, *20*, 202–207. [[CrossRef](#)]
5. Romanova, V.S.; Khotina, I.A.; Kushakova, N.S.; Kovalev, A.I.; Kharitonova, V.G.; Kupriyanova, D.V.; Naumkin, A.V. Compound based on star-shaped oligophenylene and fullerene C60. *Mendeleev Commun.* **2022**, *32*, 783–785. [[CrossRef](#)]
6. Popov, V.A.; Borunova, A.B.; Senatulin, B.R.; Shelekhov, E.V.; Kirichenko, A.N. Peculiarities of fullerenes and carbon onions application for reinforcing the aluminum matrix in the metal matrix composites. *Surf. Interface Anal.* **2019**, *52*, 127–131. [[CrossRef](#)]
7. Dhand, V.; Yadav, M.; Kim, S.H.; Rhee, K.Y. A comprehensive review on the prospects of multi-functional carbon nano onions as an effective, high-performance energy storage material. *Carbon* **2020**, *175*, 534–575. [[CrossRef](#)]
8. Volkov, D.S.; Krivoshein, P.K.; Mikheev, I.V.; Proskurnin, M.A. Pristine detonation nanodiamonds as regenerable adsorbents for metal cations. *Diam. Relat. Mater.* **2020**, *110*, 108121. [[CrossRef](#)]
9. Popov, V. Several Aspects of Application of Nanodiamonds as Reinforcements for Metal Matrix Composites. *Appl. Sci.* **2021**, *11*, 4695. [[CrossRef](#)]
10. Qin, J.-X.; Yang, X.-G.; Lv, C.-F.; Li, Y.-Z.; Liu, K.-K.; Zang, J.-H.; Yang, X.; Dong, L.; Shan, C.-X. Nanodiamonds: Synthesis, properties, and applications in nanomedicine. *Mater. Des.* **2021**, *210*, 110091. [[CrossRef](#)]
11. Parker, D.M.; Lineweaver, A.J.; Quast, A.D.; Zharov, I.; Shumaker-Parry, J.S. Thiol-terminated nanodiamond powders for support of gold nanoparticle catalysts. *Diam. Relat. Mater.* **2021**, *116*, 108449. [[CrossRef](#)]
12. Kuznetsov, V.L.; Aleksandrov, M.N.; Zagoruiko, I.V.; Chuvilin, A.L.; Moroz, E.M.; Kolomiichuk, V.N.; Likholobov, V.A.; Brylyakov, P.M.; Sakovitch, G.V. Study of ultradispersed diamond powders obtained using explosion energy. *Carbon* **1991**, *29*, 665–668. [[CrossRef](#)]
13. Leonard, K.J.; Busby, J.; Zinkle, S. Aging effects on microstructural and mechanical properties of select refractory metal alloys for space-reactor applications. *J. Nucl. Mater.* **2007**, *366*, 336–352. [[CrossRef](#)]
14. Xia, Y.; Wang, Z.; Song, L.; Wang, W.; Chen, J.; Ma, S. Inductively coupled plasma etching of bulk tungsten for MEMS applications. *Sens. Actuators A Phys.* **2022**, *345*, 113825. [[CrossRef](#)]
15. Yu, M.; Pu, G.; Xue, Y.; Wang, S.; Chen, S.; Wang, Y.; Yang, L.; Wang, Z.; Zhu, T.; Tan, T.; et al. The oxidation behaviors of high-purity niobium for superconducting radio-frequency cavity application in vacuum heat treatment. *Vacuum* **2022**, *203*, 111258. [[CrossRef](#)]
16. Lavigne, O.; Luzin, V.; Labonne, M.; Missiaen, J.-M. Neutron diffraction characterizations of NbC-Ni cemented carbides thermal residual stresses. *Int. J. Refract. Met. Hard Mater.* **2022**, *109*, 105966. [[CrossRef](#)]
17. Graboś, A.; Rutkowski, P.; Huebner, J.; Kozień, D.; Zhang, S.; Kuo, Y.-L.; Kata, D.; Hayashi, S. Oxidation performance of spark plasma sintered Inconel 625-NbC metal matrix composites. *Corros. Sci.* **2022**, *205*, 110453. [[CrossRef](#)]
18. Sanad, M.M.S.; El-Sadek, M.H. Porous niobium carbide as promising anode for high performance lithium-ions batteries via cost-effective processing. *Diam. Relat. Mater.* **2022**, *121*, 108722. [[CrossRef](#)]
19. Dai, W.; Yue, B.; Chang, S.; Bai, H.; Liu, B. Mechanical properties and microstructural characteristics of WC-bronze-based impregnated diamond composite reinforced by nano-NbC. *Tribol. Int.* **2022**, *174*, 107777. [[CrossRef](#)]
20. Zhang, W.; Jin, H.; Du, Y.; Chen, G.; Zhang, J. Sulfur and nitrogen codoped Nb₂C MXene for dendrite-free lithium metal battery. *Electrochim. Acta* **2021**, *390*, 138812. [[CrossRef](#)]
21. Arif, N.; Gul, S.; Sohail, M.; Rizwan, S.; Iqbal, M. Synthesis and characterization of layered Nb₂C MXene/ZnS nanocomposites for highly selective electrochemical sensing of dopamine. *Ceram. Int.* **2020**, *47*, 2388–2396. [[CrossRef](#)]
22. Babar, Z.U.D.; Zheng, R.-K.; Mumtaz, M.; Rizwan, S. Magneto-transport of mechanically-pressed niobium carbide (Nb₂C) distorted MXene. *Mater. Lett.* **2020**, *285*, 129210. [[CrossRef](#)]
23. Zou, Q.; Jiao, Z.; Li, Y.; He, W.; Li, S.; Luo, Y. Effects of TiC_{0.4} on microstructure and properties of WC composites. *J. Alloys Compd.* **2022**, *925*, 166588. [[CrossRef](#)]

24. Han, L.; Liu, Z.; Yu, L.; Ma, Z.; Huang, Y.; Liu, Y.; Wang, Z. Effect of WC nanoparticles on the thermal stability and mechanical performance of dispersion-reinforced Cu composites. *Scr. Mater.* **2023**, *222*, 115030. [CrossRef]
25. Shen, Q.; Ge, S.; Zhao, A.; Sun, Y.; Zhang, J.; Zhou, D.; Luo, G.; Zhang, L. Microstructural evolution and mechanical behavior of porous W reinforced by in-situ W₂C. *J. Alloys Compd.* **2019**, *797*, 1106–1114. [CrossRef]
26. Garcia-Ayala, E.; Tarancon, S.; Ferrari, B.; Pastor, J.; Sanchez-Herencia, A. Thermomechanical behaviour of WC-W₂C composites at first wall in fusion conditions. *Int. J. Refract. Met. Hard Mater.* **2021**, *98*, 105565. [CrossRef]
27. Šestan, A.; Sreekala, L.; Markelj, S.; Kelemen, M.; Zavašnik, J.; Liebscher, C.H.; Dehm, G.; Hickel, T.; Čeh, M.; Novak, S.; et al. Non-uniform He bubble formation in W/W₂C composite: Experimental and ab-initio study. *Acta Mater.* **2022**, *226*, 117608. [CrossRef]
28. Zhao, S.; Yang, L.; Huang, Y.; Xu, S. Enrichment of in-situ synthesized WC by partial dissolution of ex-situ eutectoid-structured WC/W₂C particle in the coatings produced by laser hot-wire deposition. *Mater. Lett.* **2020**, *281*, 128641. [CrossRef]
29. Tungsten Carbide. Available online: https://en.wikipedia.org/wiki/Tungsten_carbide (accessed on 1 August 2022).
30. Niobium Carbide. Available online: https://en.wikipedia.org/wiki/Niobium_carbide (accessed on 1 August 2022).
31. Ma, J.; Wu, M.; Du, Y.; Chen, S.; Jin, W.; Fu, L.; Yang, Q.; Wen, A. Formation of nanocrystalline niobium carbide (NbC) with a convenient route at low temperature. *J. Alloys Compd.* **2009**, *475*, 415–417. [CrossRef]
32. Popov, V. The impact of the diamond reinforcing particle size on their interaction with the aluminum matrix of composites in the course of heating. *Surf. Interface Anal.* **2018**, *50*, 1106–1109. [CrossRef]
33. Popov, V.; Borunova, A.; Shelekhov, E.; Cheverikin, V.; Khodos, I. Several Aspects of Interaction between Chrome and Nanodiamond Particles in Metal Matrix Composites When Being Heated. *Inventions* **2022**, *7*, 75. [CrossRef]
34. Benjamin, J.S.; Volin, T.E. The mechanism of mechanical alloying. *Met. Mater. Trans. B* **1974**, *5*, 1929–1934. [CrossRef]
35. El-Eskandarany, M.S. Fabrication of Nanocomposite Materials. In *Mechanical Alloying: For Fabrication of Advanced Engineering Materials*; Noyes Publications/William Andrew Publishing: Norwich, NY, USA, 2001; pp. 45–61. [CrossRef]
36. Jain, H.; Shadangi, Y.; Chakravarty, D.; Dubey, A.K.; Mukhopadhyay, N. High entropy steel processed through mechanical alloying and spark plasma sintering: Alloying behaviour, thermal stability, and mechanical properties. *Mater. Sci. Eng. A* **2022**, *856*, 144029. [CrossRef]
37. Lu, L.; Lai, M.O. Mechanical Alloying. In *Kluwer*; Academic Publisher: Cambridge, MA, USA, 1998; 276p.
38. Höhne, G.W.H.; Hemminger, W.F.; Flammersheim, H.-J. *Differential Scanning Calorimetry*; Springer: Berlin/Heidelberg, Germany, 2003; 298p. [CrossRef]
39. Spathara, D.; Sergeev, D.; Kobertz, D.; Müller, M.; Putman, D.; Warnken, N. Thermodynamic study of single crystal, Ni-based superalloys in the $\gamma+\gamma'$ two-phase region using Knudsen Effusion Mass Spectrometry, DSC and SEM. *J. Alloys Compd.* **2021**, *870*, 159295. [CrossRef]
40. Toda, A. Kinetics of enthalpy recovery studied by temperature-modulated differential scanning calorimetry. *Thermochim. Acta* **2022**, *716*, 179330. [CrossRef]
41. Gonçalves, R.L.; Robustillo, M.D.; Filho, P.D.A.P. A simplified two-resistance model for the description of melting curves obtained through differential scanning calorimetry. *Thermochim. Acta* **2022**, *714*, 179269. [CrossRef]
42. Couturier, L.; De Geuser, F.; Deschamps, A. A comparative study of Fe-Cr unmixing using differential scanning calorimetry and small-angle scattering. *Mater. Charact.* **2021**, *173*, 110934. [CrossRef]
43. Shelekhov, E.V.; Sviridova, T.A. Programs for X-ray analysis of polycrystals. *Met. Sci. Heat Treat.* **2000**, *42*, 309–313. [CrossRef]
44. Kwon, Y.-S.; Gerasimov, K.B.; Yoon, S.-K. Ball temperatures during mechanical alloying in planetary mills. *J. Alloys Compd.* **2002**, *346*, 276–281. [CrossRef]
45. Popov, V.A. X-ray micro-absorption enhancement for non-agglomerated nanodiamonds in mechanically alloyed aluminium matrix composites. *Phys. Status Solidi (A)* **2015**, *212*, 2722–2726. [CrossRef]
46. Wirtz, G.P.; Sis, L.B.; Wheeler, J.S. Sublimation of MoO₃ from WO₃-MoO₃ catalysts during the oxidation of toluene. *J. Catal.* **1975**, *38*, 196–205. [CrossRef]
47. Yang, Y.; Ma, Y.; Yao, J.; Loo, B. Simulation of the sublimation process in the preparation of photochromic WO₃ film by laser microprobe mass spectrometry. *J. Non-Cryst. Solids* **2000**, *272*, 71–74. [CrossRef]